

Transport properties of ion-implanted and chemically doped polyaniline films

A. N. Aleshin, N. B. Mironkov, and A. V. Suvorov

A. F. Ioffe Physico-Technical Institute, Russian Academy of Sciences, St. Petersburg 194021, Russia

J. A. Conklin

U.S. Naval Research Laboratory, Washington, D.C. 20375-5345

T. M. Su and R. B. Kaner

Department of Chemistry and Biochemistry and Solid State Science Center, University of California,

Los Angeles, California, 90095-1569

(Received 14 March 1996; revised manuscript received 5 June 1996)

The low-temperature dc conductivity and magnetoconductivity of ion-implanted (Ar^+) and chemically doped (H_2SO_4) polyaniline films have been studied. The metal-insulator transition has been observed for ion-implanted polyaniline films on increasing the irradiation dose to 3×10^{17} ions cm^{-2} . The maximum values of the room-temperature conductivity reached 800 S cm^{-1} for ion-implanted and 8 S cm^{-1} for chemically doped polyaniline films. In both cases, for samples on the insulator side of the metal-insulator transition, $\sigma(T) = \sigma(0) \exp[-(T_0/T)^m]$, where $m \sim 0.5$, whereas for the most heavily ion-implanted polyaniline films $\sigma(T) \sim T$ at $T > 20 \text{ K}$; the minimum in the $\sigma(T)$ occurs at $T \sim 20 \text{ K}$ and a negative magnetoconductance $\Delta\sigma(H, T) \sim H^2$ has been observed. It is shown that electron-electron Coulomb interactions play an important role in charge-carrier transport in ion-implanted polyaniline films near the metal-insulator transition. [S0163-1829(96)03239-0]

INTRODUCTION

Polyaniline is one of the most promising conducting polymers for applications due to its chemical and oxidative stability in both the undoped and doped forms.^{1,2} Although relatively high conductivity has been obtained for polyaniline doped with conventional protonic acids,³ the temperature dependence of the conductivity typically shows activated transport. Recently, the disorder-induced metal-insulator transition has been observed in polyaniline films doped by camphor sulfonic acid ($\text{C}_{10}\text{H}_{16}\text{O}_4\text{S}$).⁴ The conductivity of polyaniline-camphor sulfonic acid-doped films reached 400 S cm^{-1} and was nearly temperature independent.⁵ Alternatively, ion implantation is another effective method to increase the conductivity of both conjugated and nonconjugated polymers.⁶⁻⁸ The effects of ion implantation on the electrical conductivity of polyaniline have recently been studied.⁹⁻¹² The conductivities measured for ion-implanted polyaniline films are comparable to those for polyaniline doped by conventional acids.^{3,13-16} However, the transport mechanism in ion-implanted polyaniline films, especially on the metal side of the metal-insulator transition, has not been investigated thoroughly. In the present work, the electrical properties of ion-implanted and chemically doped polyaniline films over the temperature range $1.8-300 \text{ K}$ and magnetic fields up to 2.7 T are studied in order to better understand the charge-carrier transport mechanism in doped conjugated polymers.

EXPERIMENT

Polyaniline, in the emeraldine oxidation state, was prepared via chemical oxidation of aniline (Aldrich, 99.5%)

with ammonium peroxydisulfate (Fisher, reagent grade) in a hydrochloric acid (Fisher, reagent grade) medium.¹⁷ Free-standing polyaniline films ($\sim 40 \mu\text{m}$ thick) were prepared by heating a dispersion of polyaniline powder in *N*-methyl-2-pyrrolidinone (5% weight/volume) in a convection oven at $110 \text{ }^\circ\text{C}$ for 1–3 h. The base polyaniline films were chemically doped to form the conducting emeraldine salt by equilibrating the films in a $1.0M \text{ H}_2\text{SO}_4$ solution for 3–5 h, resulting in fully protonated imine nitrogens along the polyaniline backbone.

Free-standing polyaniline base films were irradiated by rastering a beam of Ar^+ ions across one surface covering a $2 \times 2.5 \text{ cm}^2$ area. The energy of the beam was maintained at 90 keV with doses ranging from 1×10^{14} to 3×10^{17} ions cm^{-2} . The ion-beam current density during irradiation ranged from 2 to $10 \mu\text{A cm}^{-2}$. The substrate temperatures during ion implantation for samples irradiated with low and intermediate doses remained below $200 \text{ }^\circ\text{C}$, which is considerably less than the crosslinking temperature for polyaniline films ($\sim 240 \text{ }^\circ\text{C}$).¹⁸ For two representative samples irradiated with the maximum dose, the substrate temperature during irradiation was raised to $200 \pm 10 \text{ }^\circ\text{C}$ and $230 \pm 10 \text{ }^\circ\text{C}$, respectively. The ion distribution and the thickness of the conductive region formed was estimated using a standard transport and range of ions in matter (TRIM) calculation.¹⁹

Four-probe conductivity was measured by attaching silver wires in a planar geometry to the implanted surface using silver paint. A computer-controlled automated measuring system, containing a helium cryostat with a superconducting magnet, was used to measure dc conductivity. The power dissipated into the samples was less than 1 mW . Temperatures were measured with a calibrated germanium resistor.

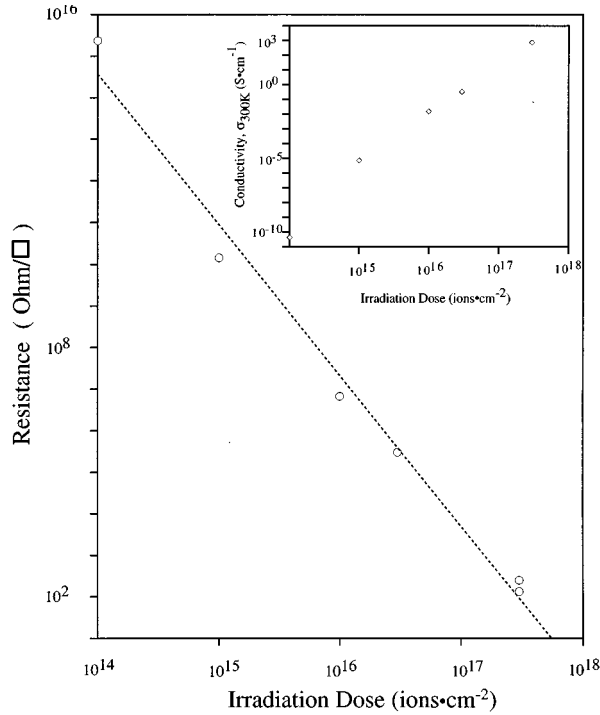


FIG. 1. Dose dependences of the sheet resistivity and the room-temperature conductivity (inset) of polyaniline films implanted with Ar^+ ions. The dotted line is a linear least-squares fit.

Magnetic fields up to 2.7 T were applied in a direction parallel to the sample surface.

RESULTS AND DISCUSSION

Figure 1 shows that irradiation of polyaniline films with Ar^+ ions decreases the room-temperature sheet resistivity from 10^{15} down to $10^2 \Omega/\square$. The values of room-temperature conductivity $\sigma(300 \text{ K})$, shown as an inset to Fig. 1, have been estimated assuming a conducting thickness of 100 nm. The depth of the conducting layer was assumed to be equal to the irradiation length. The inhomogeneity within this layer is not very high especially at low and intermediate irradiation doses according to the TRIM ion distribution profiles. From the inset to Fig. 1 it can be seen that $\sigma(300 \text{ K})$ increases up to 800 S cm^{-1} as the irradiation dose increases. This conductivity is over 12 orders of magnitude higher than $\sigma(300 \text{ K})$ before irradiation and roughly twice that of polyaniline-camphor sulfonic-acid-doped films.⁵ The chemical doping process using sulfuric acid only increases the $\sigma(300 \text{ K})$ of polyaniline films to 8 S cm^{-1} . Measurements of the thermoelectric power at 300 K show that both ion-implanted and chemically doped polyaniline films exhibit p -type conduction. Figure 2 demonstrates that an increase in the irradiation dose improves the electrical stability of ion-implanted polyaniline layers during exposure to air in comparison with a chemically doped sample. The small rise in $\sigma(300 \text{ K})$ for chemically doped polyaniline is not unexpected given the propensity for polyaniline to absorb atmospheric water, which increases the dopant mobility in the film.¹²

The temperature dependences of the conductivity of polyaniline films irradiated by Ar^+ ions with low, intermediate, and high doses are shown in Figs. 3 and 4 along with

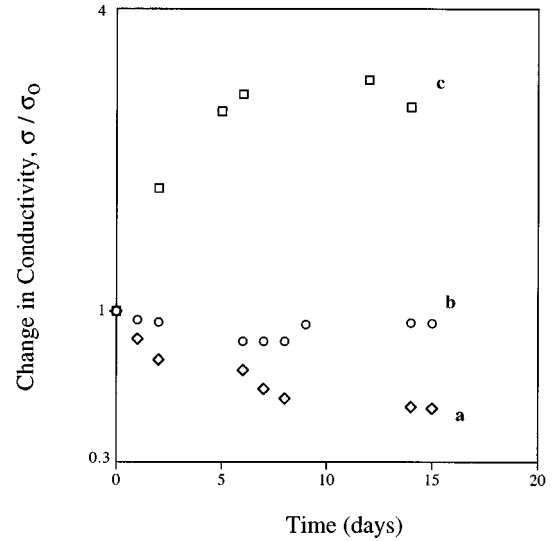


FIG. 2. Aging of ion-implanted (*a* and *b*) and chemically doped (*c*) polyaniline films during storage in air. Irradiation doses: (*a*) 3×10^{16} and (*b*) 3×10^{17} ions cm^{-2} .

a typical chemically doped sample. As can be seen by comparing Figs. 3 and 4, the increase in the irradiation dose alters the temperature dependence of the conductivity $\sigma(T)$ from activated transport to close to metallic transport, whereas the $\sigma(T)$ of chemically doped polyaniline films always has an activated nature. On the insulator side of the metal-insulator transition, $\sigma(T)$ of ion-implanted and chemically doped polyaniline films exhibits a common temperature dependence characteristic of the variable range hopping mechanism (Fig. 3):

$$\sigma(T) = \sigma(0) \exp \left[- \left(\frac{T_0}{T} \right)^m \right], \quad (1)$$

where for samples investigated $m = 0.45 - 0.66$ and $T_0 = 10^3 - 10^4 \text{ K}$.

An analysis of the temperature dependence of the dimensionless activation energy $\varepsilon(T)/kT$ in the range where $\varepsilon(T) > kT$ shows that for ion-implanted polyaniline films,

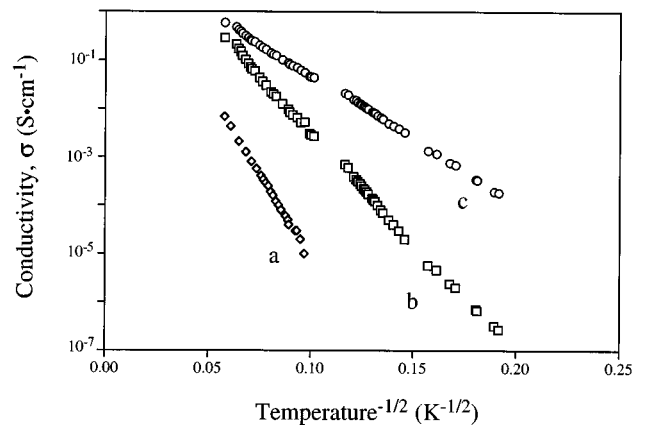


FIG. 3. Dependences of log conductivity σ versus $T^{-0.5}$ for ion-implanted (*a* and *c*) and chemically doped (*b*) polyaniline samples on the insulator side of the metal-insulator transition. Irradiation doses: (*a*) 1×10^{16} and (*c*) 3×10^{16} ions cm^{-2} .

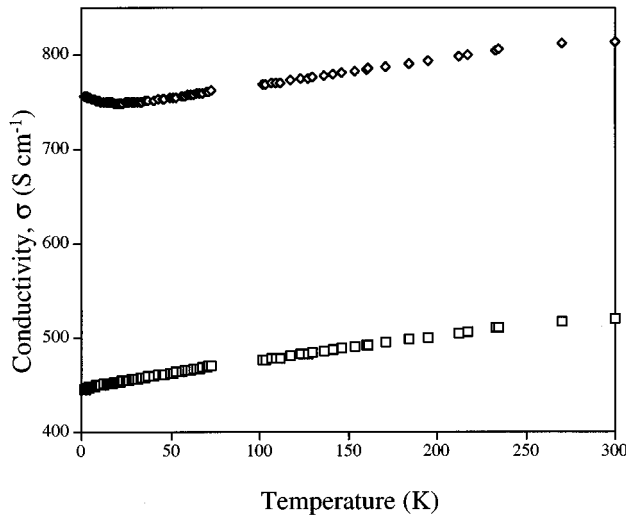


FIG. 4. Conductivity $\sigma(T)$ versus temperature for polyaniline samples, on the *metallic* side of the metal-insulator transition, ion implanted with Ar^+ at irradiation dose of 3×10^{17} ions cm^{-2} . The less metallic polyaniline (bottom) was ion implanted with a substrate temperature maintained at approximately 200 ± 10 °C, while the more metallic sample (top) had a substrate temperature of approximately 230 ± 10 °C during irradiation.

Eq. (1) with $m=0.66$ is followed at $T < 200$ K, whereas for chemically doped polyaniline films with $m=0.45$, Eq. (1) is followed over the entire temperature range. For the ion-implanted polyaniline sample (*c*) in Fig. 3 on the insulator side of the metal-insulator transition a weak positive magnetoresistance is observed from $T=77$ to 300 K; however the very high resistivity of this sample at low temperatures prevented a more sophisticated analysis.

The observed dose and temperature dependences of the conductivity indicate that in the case of ion-implanted and chemically doped polyaniline films on the insulator side of the metal-insulator transition, the main transport mechanism is charge-carrier hopping between localized states,²⁰ analogous to other conducting polymers.^{3,5,7} Recently, a $\sigma(T)$ dependence similar to that in Eq. (1) with $m \sim 0.5$ has been attributed to chemically doped polyaniline in the framework of a quasi-one-dimensional variable-range hopping model.³ However, it seems very unlikely that both chemically doped and ion-implanted polyaniline samples could be described by this common model since ion irradiation is expected to induce much more disorder. On the other hand, a recent study of transport in polypyrrole doped with PF_6^- (Ref. 21) and ion-implanted polyimide²² both indicate three-dimensional variable-range hopping in the presence of the Coulomb gap at low temperatures for samples on the insulator side of the metal-insulator transition. This model assumes electron hopping between localized states near the Fermi level with a parabolic quasigap Δ due to the Coulomb electron-electron interactions present in the single-particle density of states spectrum, while the noninteracting density of states is finite.²³ Under the one-electron transport approximation the Coulomb gap model results in conductivity obeying Eq. (1) with $m=0.5$. In this case the parameter T_0 in Eq. (1) becomes

$$T_0 = \frac{1}{k} \left(\frac{\beta e^2}{\chi \alpha} \right), \quad (2)$$

where k is the Boltzmann constant, χ is the permittivity, α is the localization radius, and $\beta=2.8$. According to this model, variable-range hopping [with $m \sim 0.5$ in Eq. (1)] should be observed at $kT < \Delta$ and the width of the quasigap can be estimated as

$$\Delta = \frac{1}{2} (T_0 T^*)^{0.5}, \quad (3)$$

where T^* is the temperature at which the power law [Eq. (1) with $m=0.5$] begins to be satisfied. For example, for the ion-implanted sample *c* shown in Fig. 3 ($T_0=3.9 \times 10^3$ K, $T^*=10^2$ K), the width of the quasigap is $\Delta=26.8$ meV. Although the values obtained for T_0 and Δ are rather large, they are not unusual for ion-implanted semiconductors. These large values indicate that the samples are well within the insulating regime and far away from the metal-insulator transition.

As mentioned above, the increase in irradiation dose leads to the observation of the metal-insulator transition in ion-implanted polyaniline layers. The temperature dependences of conductivity for the two representative highly ion-implanted polyaniline samples on the metallic side of the metal-insulator transition are shown in Fig. 4. Both samples were irradiated with the same dose 3×10^{17} ions/ cm^2 ; however, the substrate temperature during irradiation for the less metallic sample was maintained at approximately 200 ± 10 °C, while the more metallic sample had a substrate temperature of approximately 230 ± 10 °C. As indicated in Fig. 4, the estimated values of $\sigma(300$ K) for these samples, assuming a 100-nm conducting layer thickness, are typically 500–800 S cm^{-1} . The $\sigma(T)$ dependences are very weak with conductivity ratios $\sigma(300$ K)/ $\sigma(1.9$ K)=1.08–1.17, similar to the best polyaniline-camphor sulfonic-acid-doped films on the metallic side of the metal-insulator transition.⁵ For both samples in the temperature range $T > 20$ K, $\sigma(T)$ is nearly linear in T : $\sigma(T) = \sigma(0) + AT$, where $A=0.26$ and $\sigma(0) = 448$ (diamonds) and $\sigma(0) = 740$ (squares), as shown in Fig. 4. However, at lower temperatures, a different $\sigma(T)$ behavior is found for these samples. For the less metallic sample (squares) at $T_m < 20$ K, $\sigma(T)$ shows only a negative temperature coefficient to the resistivity, typical for dirty metals [see Fig. 5(b)], while for the more metallic sample (diamonds) the temperature coefficient of the resistivity changes sign from negative to positive, like in normal metals, below $T_m=20$ K, where a minimum in $\sigma(T)$ dependence is observed [see Fig. 5(a)]. The increase in conductivity below T_m is approximately 1–2 % of the room-temperature conductivity. A magnetic field of 2.7 T suppresses the positive temperature coefficient of the resistivity in $\sigma(T)$ for polyaniline, as shown in Fig. 5(a). Analogous increases in conductivity at low temperature have been observed in hexafluorophosphate (PF_6^-)-doped polypyrrole (but only under high pressure²¹) and in heavily doped semiconductors [e.g., B-doped Si (Ref. 24)], which has been attributed to the correlation effects expected in the metallic regime near the metal-insulator transition.^{25,26} Another explanation of this effect has been given for quasi-two-dimensional intercalated graphitic systems, where the increase in conductivity was attributed to a possible phase transition in these systems at low

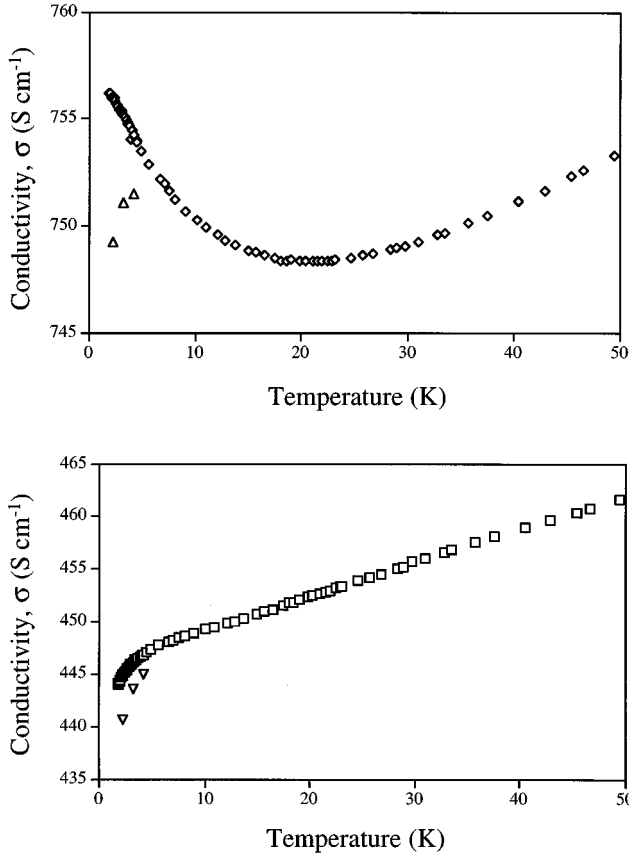


FIG. 5. Top: expanded conductivity versus temperature plot from Fig. 4 (top) below $T=50$ K, at $H=0$ (diamonds), and $H=2.7$ T (triangles). Bottom: expanded conductivity versus temperature from Fig. 4 (bottom) below $T=50$ K, at $H=0$ (squares) and $H=2.7$ T (inverted triangles).

temperatures.²⁷ It is possible that such differences in $\sigma(T)$ dependences between our two metallic samples irradiated at different temperatures indicate significant structural differences due to increasing inhomogeneity inside of the conducting layer. Nevertheless, assuming that the three-dimensional localization-interaction model near the metal-insulator transition is appropriate for ion-implanted polyaniline films, we consider that the low-temperature conductivity of the investigated layers is given by^{25,26}

$$\sigma(T) = \sigma(0) + \Delta\sigma_1(T) + \Delta\sigma_L(T) = \sigma(0) + nT^{0.5} + BT^{0.5p}, \quad (4)$$

where the second term $\Delta\sigma_1(T)$ arises from electron-electron interactions^{25,26} and the third term $\Delta\sigma_L(T)$ is the correction to the zero-temperature conductivity due to localization effects.²⁵ The temperature dependence of the localization correction is determined by the temperature dependence of the inelastic-scattering rate $\tau_{in}^{-1} = T^p$ of the dominant dephasing mechanism. For electron-phonon scattering, $p=2.5-3$; for inelastic electron-electron scattering, $p=2$ and 1.5 in the clean and dirty limits, respectively.²⁴ A recent calculation gives $p=1$ very near the metal-insulator transition.²⁸

An analysis of the low-temperature dependences of conductivity, for both polyaniline samples, in the metallic regime [Figs. 5 (top) and 5 (bottom)] shows that the curves

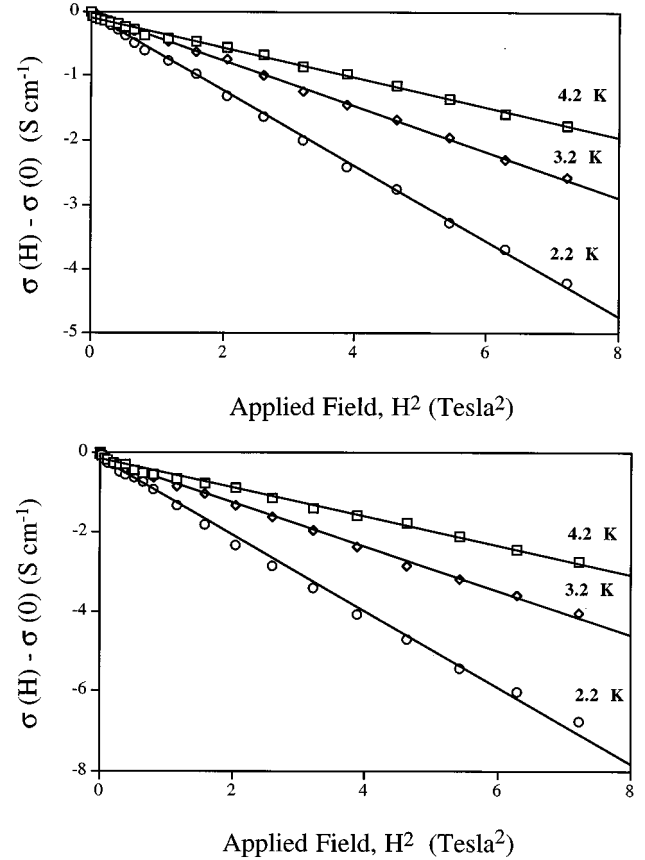


FIG. 6. Magnetoconductance versus applied field H^2 at 2.2, 3.2, and 4.2 K, for the ion-implanted polyaniline samples from Fig. 4, where the top sample is more metallic and the bottom sample is less metallic.

observed can be described by Eq. (4). The best fit for $T > T_m$ yields $p=2.03 \pm 0.11$ and $B=0.39 \pm 0.10$ for the less metallic sample [Fig. 5 (bottom)] and $p=2.88 \pm 0.14$ and $B=0.23 \pm 0.18$ for the more metallic sample [Fig. 5 (top)]. The values of n and $\sigma(0)$ are strongly dependent on magnetic field, which decreases $\sigma(0)$ and suppresses the positive temperature coefficient of resistivity for the sample in Fig. 5(a), analogous to the case of doped polypyrrole films.²¹ The exponent $p=2.88$ of the localization correction term in Eq. (4) implies that above $T=T_m$, inelastic electron-phonon scattering is dominant.²⁵

The low field magnetoconductance data [Figs. 6(a) and 6(b)] show that for both metallic polyaniline samples at $T < 4.2$ K the magnetoconductance is negative and linear in H^2 independent of the sign of the temperature coefficient of the resistivity. This can be explained by assuming that the contributions to magnetoconductance that arise from electron-electron interactions and ‘‘antilocalization’’ are of the same sign and additive.^{24,29} Usually in disordered systems the localization effects lead to positive magnetoconductance due to inelastic scattering processes. However, according to the theory of weak localization negative magnetoconductance can take place when the spin-orbit scattering is strong,²⁶ whereas electron-electron interactions always lead to negative magnetoconductance proportional to H^2 .²⁵ In this case the total low-field ($g\mu H \ll kT$) magnetoconductance is given by

$$\begin{aligned} \Delta\Sigma(H, T) = & \Delta\Sigma_I(H, T) + \Delta\Sigma_L(H, T) = \\ & -0.041 \eta \left(\frac{g\mu}{d} \right)^2 \gamma F_\sigma T^{-1.5} H^2 - \left(\frac{1}{48} \pi^2 \right) \\ & \times \left(\frac{e}{\hbar} \right)^2 G_0 (L_{\text{in}})^3 H^2. \end{aligned} \quad (5)$$

The first term on the right-hand side is the contribution due to electron-electron interactions, the second term is the contribution due to antilocalization, η and γF_σ are the interaction parameters,²⁵ $G_0 = (e^2/\hbar)$, and L_{in} is the inelastic-scattering length.

Similar magnetoconductance behavior has been observed in doped semiconductors²⁴ and conducting polymers both chemically doped⁵ and ion implanted.³⁰ In our case the separation of contributions from electron-electron interactions and localization effects is rather difficult because of the unusual temperature dependences of the conductivities of the metallic samples. On theoretical grounds, spin-orbit effects in conducting polymers should be rather weak in comparison to electron-electron interactions. So the observed strong dependences of n and $\sigma(0)$ in Eq. (4) on the magnetic field and strong negative magnetoconductance proportional to H^2 allows us to assume that the contribution from the electron-

electron interaction is probably dominant in comparison to the weak localization term in this temperature range. However, the influence of the weak localization contribution could become more apparent at lower temperatures, suggesting that further transport studies in the lower-temperature range are needed to get a more complete understanding of the transport phenomena in ion-implanted polyaniline.

CONCLUSIONS

The metal-insulator transition has been observed in polyaniline films irradiated with Ar^+ ions. The maximum value of the room-temperature conductivity of ion-implanted polyaniline films reaches 800 S cm^{-1} , at an irradiation dose of $3 \times 10^{17} \text{ ions cm}^{-2}$ and a substrate temperature of $230 \text{ }^\circ\text{C}$. Lower doses give rise to lower conductivities. The effects of electron-electron Coulomb interactions play an important role in charge-carrier transport in ion-implanted polyaniline films on both the insulator and the metallic sides of the metal-insulator transition.

ACKNOWLEDGMENT

This work was partially supported by the U.S. Office of Naval Research Grant No. N00014-93-1-1307.

- ¹Y. Cao, P. Smith, and A. J. Heeger, in *Conjugated Polymeric Materials*, Vol. 82 of *NATO Advanced Study Institute, Series E: Applied Science*, edited by J. L. Bredas and R. R. Chance (Kluwer Academic, Dordrecht, 1990).
- ²A. G. MacDiarmid and A. J. Epstein, in *Science and Applications of Conducting Polymers*, edited by W. R. Salaneck, D. T. Clark, and E. J. Samuelson (Hilger, Bristol, 1991), p. 117.
- ³Z. H. Wang, E. M. Scherr, A. G. MacDiarmid, and A. J. Epstein, *Phys. Rev. B* **45**, 4190 (1992).
- ⁴Y. Cao, P. Smith, and A. J. Heeger, *Synth. Met.* **48**, 91 (1992).
- ⁵M. Reghu, C. O. Yoon, D. Moses, A. J. Heeger, and Y. Cao, *Phys. Rev. B* **48**, 17 685 (1993).
- ⁶T. H. Loh, R. V. Oliver, and P. Sioshansi, *Nucl. Instrum. Methods Phys. Res. Sect. B* **34**, 337 (1988).
- ⁷A. N. Aleshin, A. V. Gribanov, A. V. Dobrodumov, A. V. Suvorov, and I. S. Shlimak, *Fiz. Tverd. Tela (Leningrad)* **31**, 12 (1989) [*Sov. Phys. Solid State* **31**, 6 (1989)]; *Solid State Commun.* **71**, 85 (1989).
- ⁸A. Moliton, B. Lucas, C. Moreau, R. H. Friend, and B. Francois, *Philos. Mag. B* **69**, 1155 (1994).
- ⁹J.-L. Zhu, Z.-M. Liu, Z.-W. Yu, Y.-P. Guo, Z.-T. Ma, and R.-Z. Beng, *Nucl. Instrum. Methods Phys. Res. Sect. B* **91**, 469 (1994).
- ¹⁰W. Wang, S. Lin, J. Bao, T. Rong, H. Wan, and J. Sun, *Nucl. Instrum. Methods Phys. Res. Sect. B* **74**, 514 (1993).
- ¹¹Z.-S. Tong, M.-Z. Wu, J.-L. Ding, Q.-H. Hu, M. Zhu, L. Chen, Z.-L. Xu, M.-X. Wang, and H.-X. Zhou, *Nucl. Instrum. Methods Phys. Res. Sect. B* **71**, 26 (1992).
- ¹²Y. P. Feng, D. S. Robey, Y. Q. Wang, and R. E. Giedd, *Mater. Lett.* **17**, 167 (1993).
- ¹³A. G. MacDiarmid and A. J. Epstein, *Faraday Discuss. Chem. Soc.* **88**, 317 (1989).
- ¹⁴J. C. Chiang and A. G. MacDiarmid, *Synth. Met.* **13**, 193 (1986); **13**, 193 (1986).
- ¹⁵A. G. MacDiarmid, J. C. Chiang, M. Halpern, W. S. Huang, S. L. Mu, N. L. D. Somasiri, W. Wu, and S. I. Yaniger, *Mol. Cryst. Liq. Cryst.* **121**, 173 (1985).
- ¹⁶J. P. Travers, J. Chroboczek, F. Devereux, F. Genoud, M. Nechtshein, A. Syed, E. M. Geniew, and C. Tsintavis, *Mol. Cryst. Liq. Cryst.* **121**, 195 (1985).
- ¹⁷A. G. MacDiarmid, J. C. Chiang, A. F. Richter, N. L. D. Somasiri, and A. J. Epstein, in *Conducting Polymers*, edited by L. Alacer (Reidel, Dordrecht, 1987), p. 105.
- ¹⁸J. A. Conklin, S.-C. Huang, S.-M. Huang, and R. B. Kaner, *Macromolecules* **28**, 6522 (1995).
- ¹⁹J. F. Ziegler, J. P. Biersack, and V. Littmark, *The Stopping and Range of Ions in Solids* (Pergamon, Oxford, 1985), p. 202.
- ²⁰N. F. Mott and E. A. Davis, *Electronic Processes in Non-Crystalline Materials* (Oxford University Press, Oxford, England, 1979).
- ²¹C. O. Yoon, M. Reghu, D. Moses, and A. J. Heeger, *Phys. Rev. B* **49**, 10 851 (1994).
- ²²A. N. Aleshin and A. V. Suvorov, *Philos. Mag. B* **65**, 783 (1992).
- ²³B. I. Shklovskii and A. L. Efros, *Electric Properties of Doped Semiconductors* (Springer-Verlag, Berlin, 1980).
- ²⁴P. Dai, Y. Zang, and M. P. Sarachik, *Phys. Rev. B* **45**, 3984 (1992); **46**, 6724 (1992).
- ²⁵P. A. Lee and T. V. Ramakrishnan, *Rev. Mod. Phys.* **57**, 287 (1985).
- ²⁶B. L. Altshuler, A. G. Aronov, A. I. Larkin, and D. E. Khmel'nitskii, *Zh. Eksp. Teor. Fiz.* **81**, 768 (1981) [*Sov. Phys. JETP* **54**, 411 (1981)]; B. L. Altshuler and A. G. Aronov, in *Electron-Electron Interactions in Disordered Systems*, edited by

- A. L. Efros and M. Pollak (North-Holland, Amsterdam, 1985).
- ²⁷L. Piraux, V. Bayot, J. P. Issi, M. S. Dresselhaus, M. Endo, and T. Nakajima, Phys. Rev. B **41**, 4961 (1990).
- ²⁸D. Belitz and K. I. Wysokinski, Phys. Rev. B **36**, 9333 (1987).
- ²⁹T. F. Rosenbaum, R. M. F. Milligan, G. A. Thomas, P. A. Lee, T. V. Ramakrishnan, R. N. Bhatt, K. DeConde, H. Hess, and T. Perry, Phys. Rev. Lett. **47**, 1758 (1981).
- ³⁰A. N. Aleshin, N. B. Mironkov, and A. V. Suvorov, Fiz. Tverd. Tela (St. Petersburg) **38**, 133 (1996) [Phys. Solid State **37**, 131 (1996)].